– SUPPLEMENTAL MATERIAL –

Transmitter unit

Temperature regulation

Piezo controller

PZM
PM
QD
L_1
L_2
F
M_1
FM$_2$
BS
S
PM
Xe-arc
FM$_1$
GAL
LLO
purge

open-path
through chamber

chamber wall

~ 19.5(7) m

Receiver unit

Temperature regulation

FM$_3$
purge
M_2
UV-FM
FM$_4$
L_3

chamber wall
(Teflon)

Monochromator

1200
lines/mm

FB

CCD

BS:	Beamsplitter
FB:	Circular-to-rectangular fiber bundle
S:	Shutter
L_i:	Achromatic lens
F:	Bandpass interference filter (348-392 nm)
M_i:	Highly reflective spherical (cavity) mirror
UV-FM:	UV-enhanced flat mirror
LLO:	Low loss optic
GAL:	Green alignment laser
FM$_i$:	Flat aluminium mirrors
PM:	Parabolic mirrors (off-axis)
PZM:	Piezo mirror
QD:	Quadrant photo-detector

Figure S1: Schematic of the experimental IBBCEAS setup at the atmospheric simulation chamber SAPHIR at Jülich, Germany. The cavity mirrors (M_i) have a radius of curvature of $r = -21$ m and a diameter of 40 mm (Layertec GmbH). The mirror separation was $l = 20.4 \pm 0.1$ m and the effective sample length inside the cavity was $d = 19.5(7)$ m. The mirrors were purged with zero air at a flow rate of 1.7 SLPM. The light transmitted by the cavity was collected with an achromatic lens and coupled into a multimode quartz fibre bundle (FB, circular to rectangular), which was connected to a polychromator (Shamrock 303i, grating 1200 lines mm^{-1}, spectral resolution 0.21 nm) inside the receiver unit. The dispersed light was then detected by a cooled back-illuminated charged coupled device (CCD, Andor Newton).
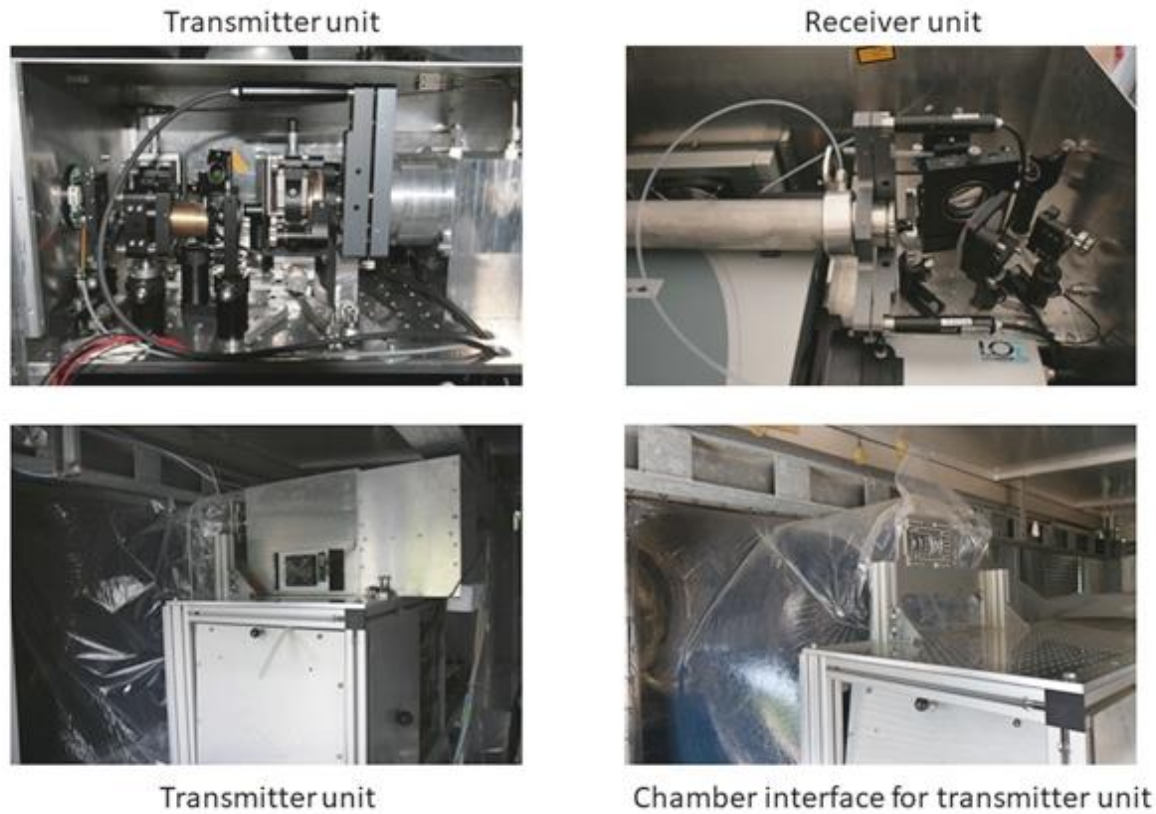
Figure S2: Photographs of the interior of the transmitter unit (upper left) and receiver unit (upper right), the mounting position of the transmitter unit on top of a frame bolted to a massive concrete support bench (lower left), and interface plate on the pressurized Teflon chamber foil before installation of the transmitter unit (lower right).
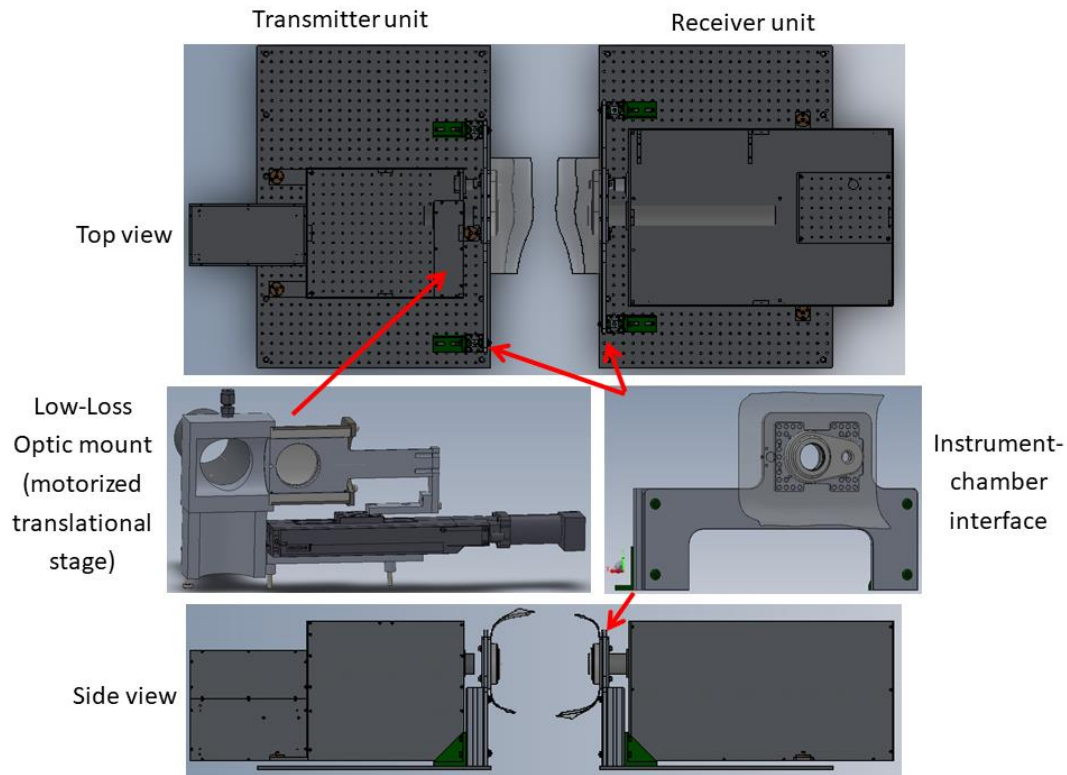
Figure S3: Upper Panel: Drawings of the top view of the transmitter and receiver units schematically. The low loss optic mount was installed inside the transmitter unit. Middle panel (left): Low loss optic mount on translational stage. While not in use the low loss optic was completely enclosed. The mount was also purged with zero air. Middle Panel (right): Drawing of the plates with feedthrough holes that were used to interface the units to the chamber (walls). Lower Panel: Drawings of the side view of the transmitter and receiver units schematically. The interface to the chamber is also shown on both sides.
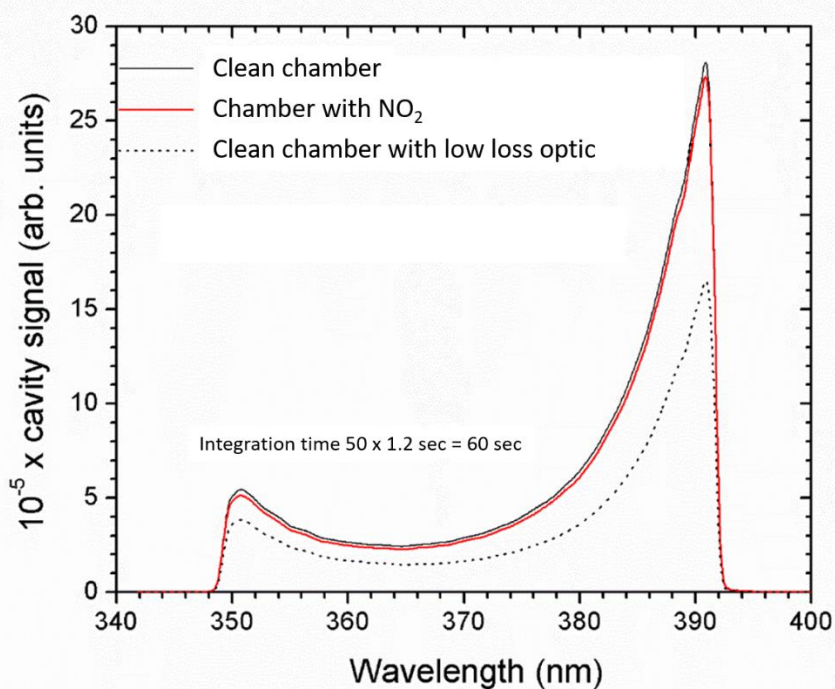
Figure S4: Examples of transmission spectra of the long cavity for a total integration time of 1 min. The signal below ~350 nm and above ~390 nm was suppressed by a single bandwidth filter (Semrock FF01-370/36) with cut-on and cut-off wavelength of 348 nm and 392 nm respectively. Gray trace: $I_0(\lambda)$, intensity transmitted by the cavity for a chamber that was flushed overnight with zero air (clean chamber). Red line: $I(\lambda)$, intensity transmitted by the cavity for a chamber that was primed with NO_2 in a reflectivity calibration measurement. Dashed line: Same as gray trace, but with the low loss optic in the beam.
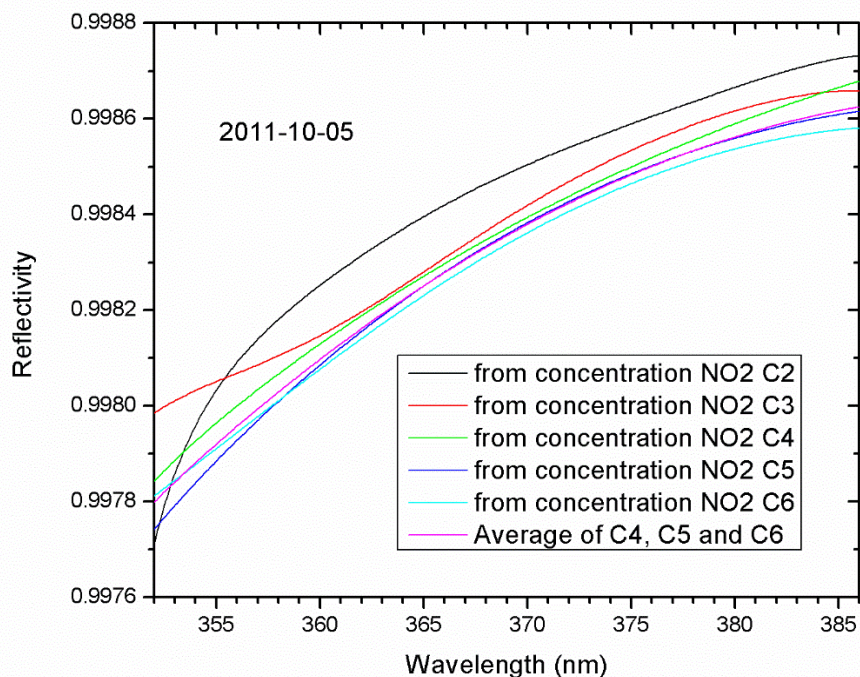
Figure S5: Reflectivity spectra, $R(\lambda)$, for 5 different concentrations (C2…C6) of NO_2 during the measurement on 5 October 2011. The trace in magenta shows the average of three measurements with different concentrations, which was used to establish the reflectivity spectrum of the mirrors.
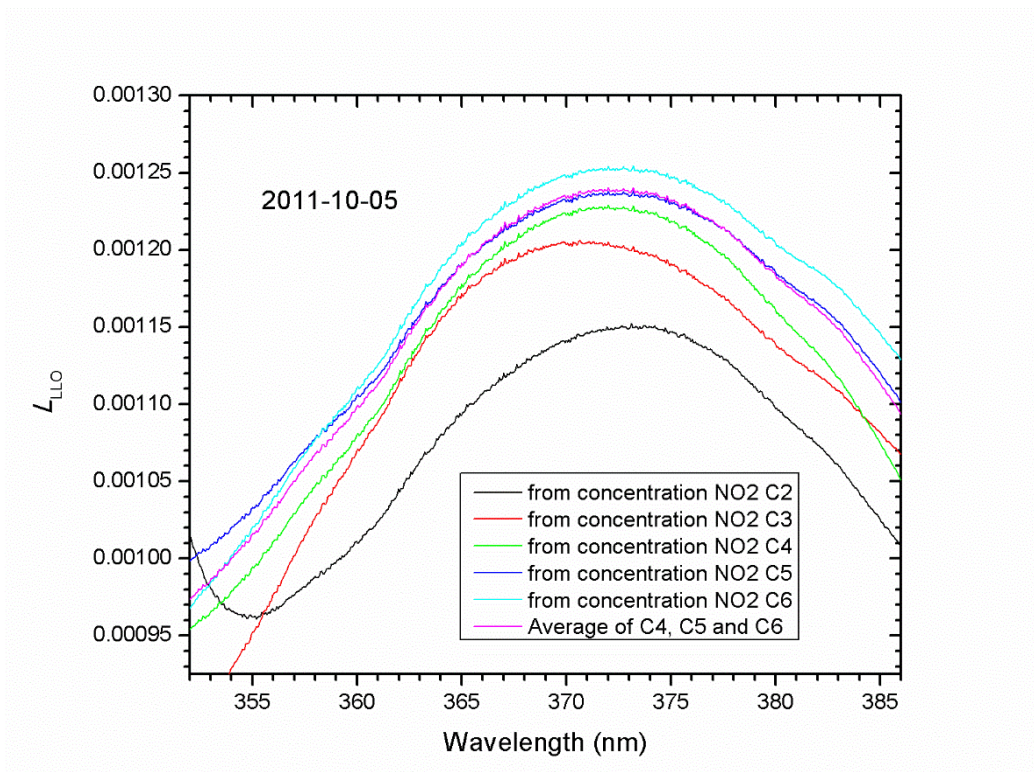
Figure S6: Example of a loss spectrum, L_{LLO} (λ), of an antireflection coated optic ("low loss optic", LLO), used to determine the reflectivity in the morning after flushing the chamber (see Figure S4). The loss was calibrated from measurements with NO₂ at different concentrations (see Figure S5). The trace in magenta shows the average of three measurements with different concentrations, which was used to establish the loss spectrum of the LLO.
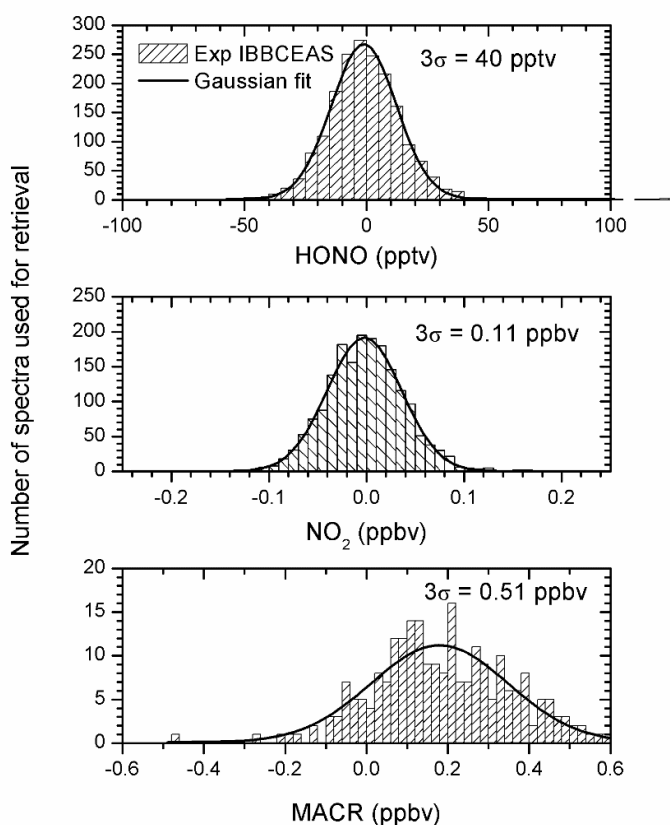
Figure S7: Establishment of the 3σ limit of detection (LOD) of the IBBCEAS instrument for a 1 min acquisition time. From the 1σ standard deviation of the residuals of individual spectral fits the distribution of deviations was established from which the LOD was

determined to be ~39 pptv for HONO, ~114 pptv for NO_2, and ca. 510 pptv for MACR in the 352-386 nm wavelength range used for the fit.
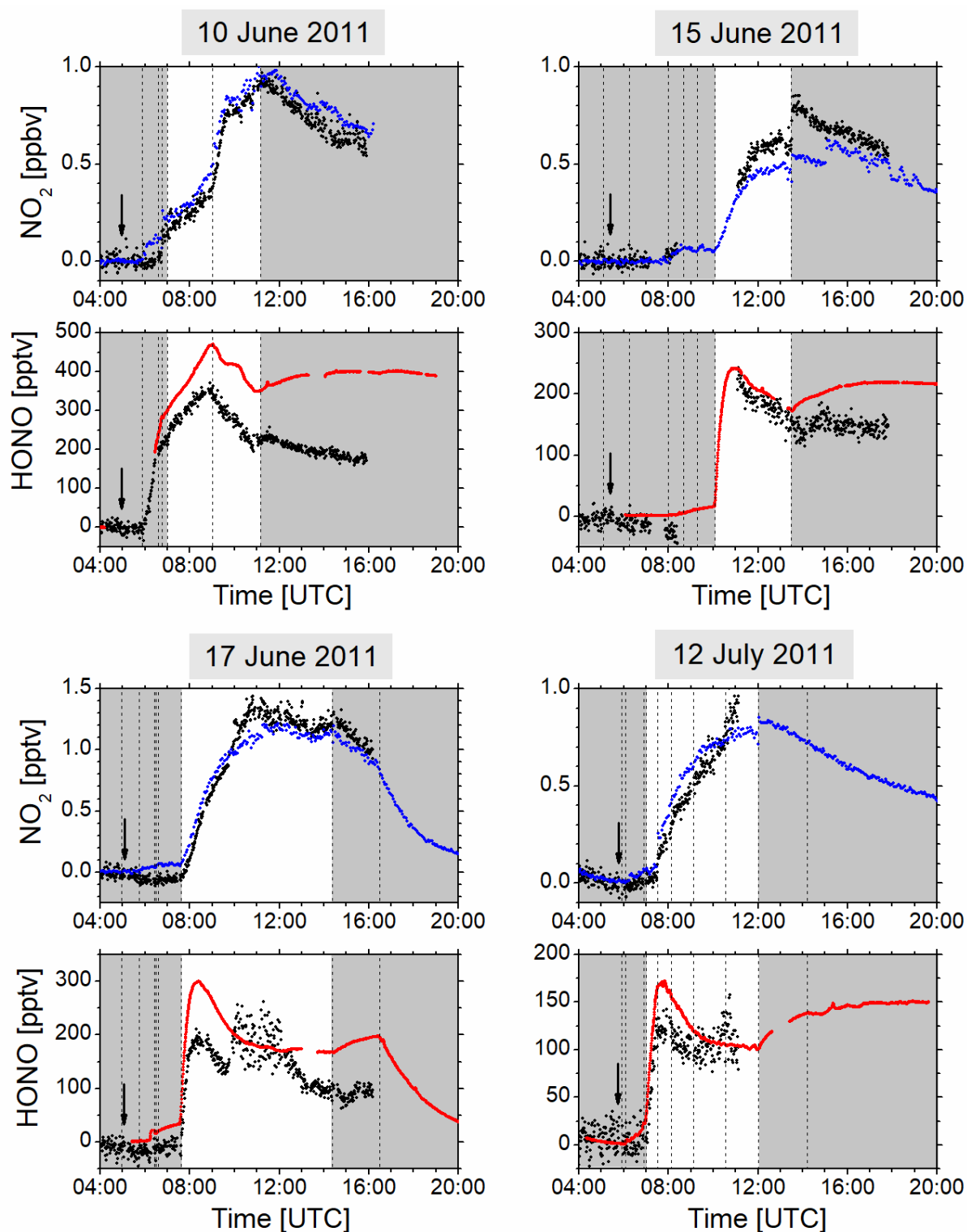
Figure S8:

10 June 2011: Start of humidification (5:55), end of humidification (6:35), O_3 addition (6:45), roof opened (7:00), isoprene addition (9:00), roof closed (11:12) – upper left two panels.

15 June 2011: Flushing of chamber stopped (5:05), isoprene addition (6:15), start of humidification (8:00), end of humidification (8:38), O_3 addition (9:15), roof opened (10:05), roof closed (13:30) – upper right two panels.

17 June 2011: Flushing of chamber stopped (04:58), start of humidification (05:45), end of humidification (06:25), O_3 addition (06:30), CO addition (06:35), roof opened (07:36), roof closed (14:23), flushing of chamber started (16:29) – lower left two panels.

12 July 2011: Flushing of chamber stopped (05:55), start of humidification (06:05), end of humidification (06:55), roof opened (07:00), 40 ppb O_3 (07:30), isoprene (08:08), isoprene (09:08), isoprene (10:33), roof closing (12:00), ventilator off (14:13) – lower right two panels.

The vertical black arrows indicate the times when measurements of I_0 in the "clean chamber" were taken. Grey area = dark conditions, white area = light-filled chamber; IBBCEAS data (black), LOPAP (red), CLS (blue).